Realistic 3D Bidomain Model of Whole Heart Electrical Activity and ECG Generation

Siniša Sovilj[1], Ratko Magjarević[1], Nigel Lovell[2], Socrates Dokos[2]

[1]University of Zagreb, Faculty of Electrical Engineering and computing, Zagreb, Croatia
[2]University of New South Wales, Graduate School of Biomedical Engineering, Sydney, Australia

Abstract

This study describes an anatomically realistic 3D bidomain model of whole-heart electrical activity. The heart was embedded in a human torso, incorporating spontaneous activation of the sinoatrial node and including conduction through the specialized conduction pathways with heterogeneous action potential (AP) morphologies throughout the heart. The model was able to generate realistic ECG waveforms, and is proposed as a useful tool for investigating the effects of altered myocardial electrical properties on the ECG.

1. Introduction

Mathematical modelling of cardiac electrical activity is performed from the cell, tissue and organ levels through to the body surface level, formulating the forward problem of the whole-organ system within the body [1].

The goal of biophysically-based modelling of cardiac function is the development of an explanatory and predictive tool in general, with a recent tendency to shift towards patient and pathology-specific heart modelling. Benefits range from predicting the effects of intervention of medical treatments, to providing the only conceivable alternative to animal experimentation [1].

In modelling the complex whole-heart within body system, in addition to accurate geometric reconstruction, there are several scale-specific biophysical modelling steps: cell modelling, tissue modelling, whole-heart modelling and organ in the body modelling. To simplify this very complex system, most investigators adopt a bidomain framework with two continuum (volume-averaged), interpenetrating domains: intracellular and extracellular domains, and third passive extramyocardial region for modelling the torso [1-3]. Today, the state-of-the-art in computational cardiac modelling and simulation is oriented to personalized, problem-specific, highly detailed, but still ventricular-only or atria-only models. Generalized, inclusive whole-heart electrical activity models embedded in the torso, with spontaneous activation and ECG generation, are relatively rare [4, 5].

2. Methods

The anatomically-realistic 3D model geometry (Figure 1, 3) was assembled from segmented CT images obtained from the Visual Human Project male dataset (http://www.nlm.nih.gov/research/visible/) (Figure 2), with the resulting mesh imported into the Comsol Multiphysics (COMSOL AB, Switzerland) finite element solver (Figure 4). Due to computational simplicity, we used modified FitzHugh–Nagumo (FHN) equations to simulate action potentials in different regions of the heart.

The governing equation for the extracellular voltage V in the passive volume conductor regions (excluding the myocardium) was given by the Laplace formulation

$$\nabla \cdot \left(-\sigma_o \nabla V \right) = 0$$

where σ_o is the electrical conductivity of respective outside-heart domains: torso, lungs and cardiac blood chambers, with values given in Table 1 [3, 6]. All exterior boundaries of the torso were set to be electrically insulating (zero normal component of current density), and all interior boundaries in contact with the heart were set to $V=V_e$ where V_e is the extracellular voltage in the myocardial walls.

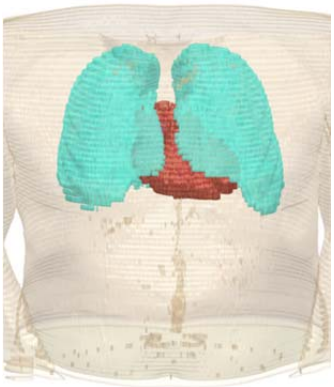

Figure 1. Geometry of the model. Whole-heart geometry including atrial and ventricular cavities is shown embedded in the torso with lungs.

The heart itself was divided into seven subdomains or regions with heterogeneous cardiac cell properties and tissue conductivities representing specialized cells of the conduction system and the myocardium. An electrical isolation gap exists between the atria and ventricles except at a junction in the septum that links the atrioventricular node (AVN) with the His bundle (Figure 2).

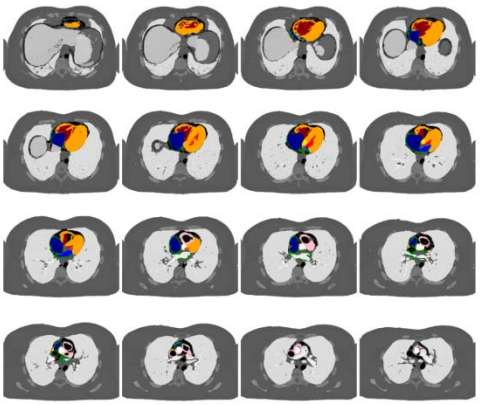

Figure 2. Segmented CT images of the heart regions, lungs and torso.

Table 1. Electrical conductivity values for model tissues.

Subdomain	Conductivity (S/m) [6]	Conductivity (S/m) [3]	Conductivity (S/m) Present study
Heart	0.054	0.400*[c] 0.179*[d]	0.05
Blood	0.7	0.625	0.7
Lungs	0.203*[a] 0.039*[b]	0.050	0.04
Muscle	0.202	0.526*[e] 0.076*[f]	N/A
Fat	0.012	0.040	N/A
Bone	0.000975*[g]	0.006	N/A
Torso	N/A	N/A	0.2

*a deflated, *b inflated, *c longitudinal, *d transversal, *e parallel, *f normal, *g marrow.

The bidomain model of cardiac activation, including the SAN, was defined at the cellular level by three dependent variables: V_e – the extracellular potential, V_i – the intracellular potential, and u – a recovery variable governing cellular refractoriness. The bidomain equations were based on modified FitzHugh-Nagumo equations [7, 8]. For the each region of the heart they were defined according to:

$$\frac{\partial V_e}{\partial t} - \frac{\partial V_i}{\partial t} + \nabla \cdot \left(-\sigma_e \nabla V_e\right) = i_{ion}$$

$$\frac{\partial V_i}{\partial t} - \frac{\partial V_e}{\partial t} + \nabla \cdot \left(-\sigma_i \nabla V_i\right) = -i_{ion}$$

$$\frac{\partial u}{\partial t} = ke\left[\frac{\left(V_m - B\right)}{A} - du - b\right]$$

with σ_e, σ_i denoting the extracellular and intracellular conductivities respectively, $V_m = V_i - V_e$, and a, b, c_1, c_2, d, e, k, A, B are region-specific parameters, whilst i_{ion} is defined according to:

$$i_{ion} = kc_1\left(V_m - B\right)\left[a - \frac{\left(V_m - B\right)}{A}\right]\left[1 - \frac{\left(V_m - B\right)}{A}\right] + kc_2 u$$

within the SAN and

$$i_{ion} = kc_1\left(V_m - B\right)\left[a - \frac{\left(V_m - B\right)}{A}\right]\left[1 - \frac{\left(V_m - B\right)}{A}\right] + kc_2 u\left(V_m - B\right)$$

within the walls of the atria, ventricles, AVN, His bundle, bundle branches and Purkinje fibers. Parameters of the model with region-specific values, along with initial variable values are listed in Table 2.

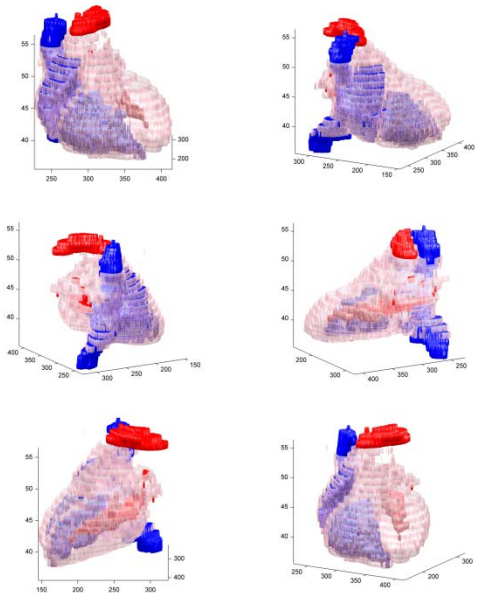

Figure 3. Heart geometry showing atrial and ventricular cavities.

Table 2. Model parameters and initial values by region.

	SAN	ATR	AVN	HIS	BNL	PKJ	VEN
a	-0.60	0.13	0.13	0.13	0.13	0.13	0.13
b	-0.30	0	0	0	0	0	0
c_1	1000	2.6	2.6	2.6	2.6	2.6	2.6
c_2	1.0	1.0	1.0	1.0	1.0	1.0	1.0
d	0	1	1	1	1	1	1
e	0.0660	0.0096	0.0132	0.0050	0.0022	0.0047	0.0056
A	0.033	0.280	0.280	0.280	0.280	0.280	0.280
B	-0.022	-0.085	-0.085	-0.085	-0.085	-0.085	-0.085
k	1000	1000	1000	1000	1000	1000	1000
σ_e	0.5	8	0.5	10	15	35	8
σ_i	0.5	8	0.5	10	15	35	8
V_i	-0.06	-0.085	-0.085	-0.085	-0.085	-0.085	-0.085
V_e	0	0	0	0	0	0	0
u	0	0	0	0	0	0	0

Boundary conditions on all interior boundaries in contact with the torso, lungs and cardiac cavities are zero-flux for V_i, therefore $-\mathbf{n}\cdot\boldsymbol{\Gamma}=0$ where $\mathbf{n}$ is the unit outward normal vector on the boundary, and $\boldsymbol{\Gamma}$ is the flux vector through that boundary for the intracellular voltage, equal to $\boldsymbol{\Gamma}=-\sigma_i\cdot\partial V_i/\partial\mathbf{n}$. For the variable V_e, the inward flux on these boundaries is equal to the outward current density $\mathbf{J}$ from the torso / chamber volume conductor, therefore $-\sigma_e\cdot\partial V_e/\partial\mathbf{n}=\mathbf{n}\cdot\mathbf{J}$.

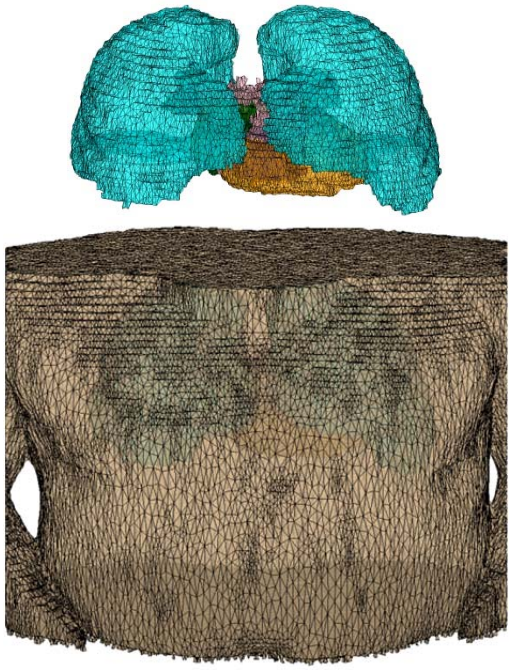

Figure 4. Finite element mesh layout for the heart and lungs embedded in the torso.

The realistic mesh geometry (Figure 4) incorporated the whole-heart as a volume current source, with heart cavities, lungs and torso as passive volume conductors. We placed four surface electrodes at the limbs of the torso: V_R (right arm), V_L (left arm), V_F (left leg) and V_{GND} (right leg or ground) to simulate the Einthoven leads of a standard 12-lead system (Figure 5).

The resulting finite element mesh consisted of 298,728 tetrahedral elements with 682,768 degrees of freedom. The simulations were performed on an Intel Core i7-970 processor workstation with 24 GB of memory, 2x6 cores and processing power of about 100 Gflops.

3. Results

The model was able to simulate and generate realistic electrocardiogram (ECG) morphologies under normal and pathological heart states (Figure 5). The time dependent solver took about 12 hours to solve 1 simulated second of ECG with 1 ms resolution (Figure 6).

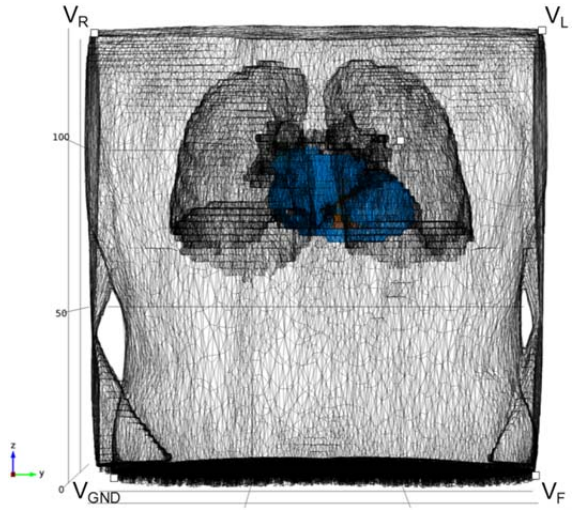

Figure 5. Simulation of heart electrical activity with position of electrodes.

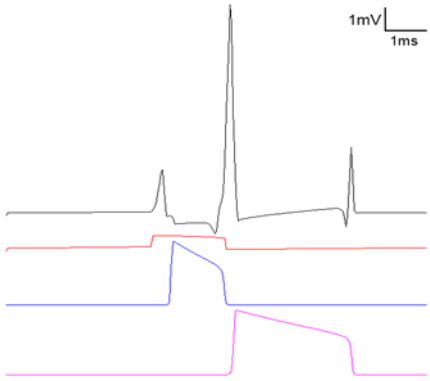

Figure 6. Simulated lead II ECG and action potentials of: SAN, atria and ventricles.

4. Conclusion

An anatomically-realistic 3D cardiac model was developed using available commercial finite element software that could run on relatively standard computer hardware. In addition to its educational value, we believe the model has further research and application potential and can be used as a simulator for various arrhythmias including atrial /ventricular fibrillation, as well as able to simulate the effects of changes in tissue conductivity, AP duration or AP shape on ECG morphology, with the aim of developing new diagnostic ECG algorithms, methods and tools [9]. As a continuous bidomain model, it also allows simulation of defibrillation.

In the future work, the model could be improved with finer geometry resolution and further anatomical details. Also, with patient-specific geometry and body surface potentials, cardiac electrical function could be inversely assessed, more detailed cell models could be used and eventually the model could be improved by coupling with other electro-mechanical and blood flow models.

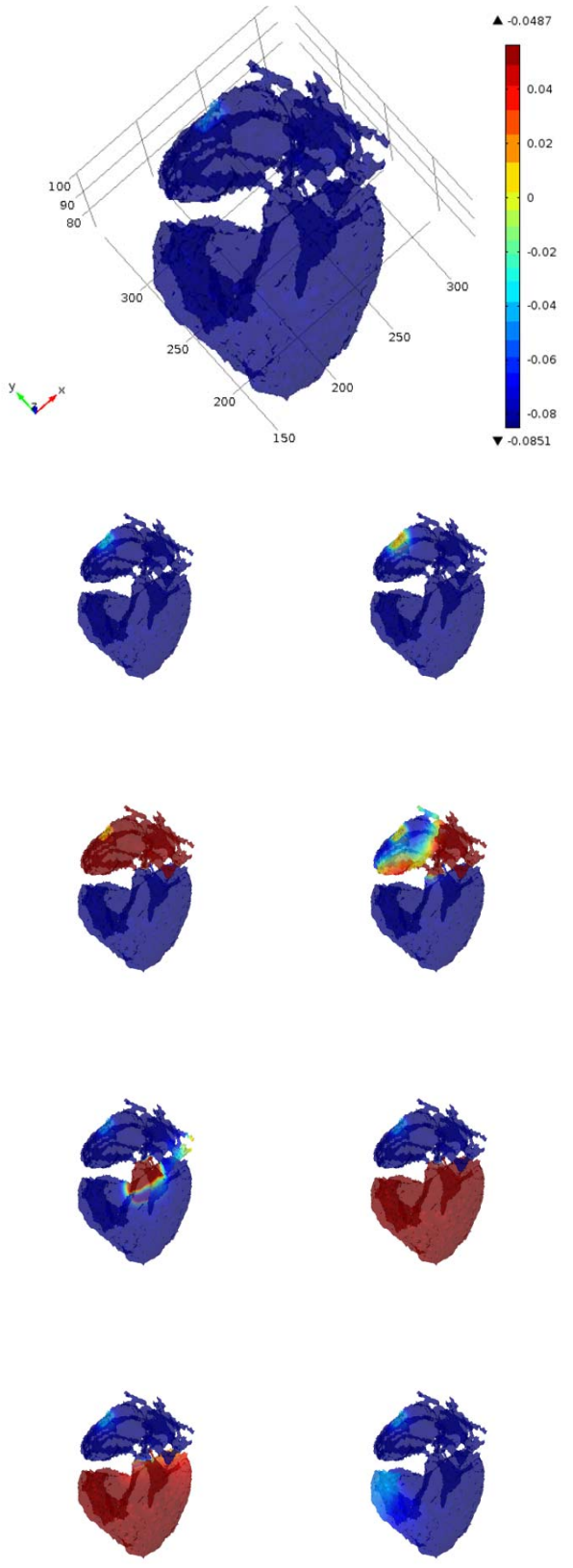

Figure 7. Top view of the heart electrical activity in 200 ms time steps.

Acknowledgements

This study was supported by the Australian Department of Education, Employment and Workplace Relation (DEEWR) and the Ministry of Science, Education and Sport (MZOS) of the Republic of Croatia, under grant #036-0362979-1554. During the academic visit SS was holding an Australian Government's Endeavour Award fellowship (#ERF_PDR_3203_2012) for postdoctoral research at the University of New South Wales, Graduate School of Biomedical Engineering.

References

[1] Pullan AJ, Buist ML, Cheng LK. Mathematically modelling the electrical activity of the heart - From Cell to Body Surface and Back Again: World Scientific; 2005.

[2] Jacquemet V, van Oosterom A, Vesin J-M, Kappenberger L. Analysis of electrocardiograms during atrial fibrillation. Engineering in Medicine and Biology Magazine, IEEE 2006;25:79-88.

[3] Malmivuo J, Plonsey R. Bioelectromagnetism: principles and applications of bioelectric and biomagnetic fields. Oxford University Press; 1995.

[4] Pfeifer B, Seger M, Hanser F, Hintermüller C, Mühlthaler M, Tilg B. A training whole-heart model for simulating propagation and ECG patters. Biomedical Signal Processing and Control 2007;2:323-30.

[5] Trayanova NA. Whole-heart modeling - Applications to cardiac electrophysiology and electromechanics. Circulation Research 2011;108:113-28.

[6] Gabriel S, Lau RW, Gabriel C. The dielectric properties of biological tissues: II. Measurements in the frequency range 10 Hz to 20 GHz. Physics in Medicine and Biology 1996;41:2251-69.

[7] Sovilj S, Magjarevic R, Al Abed A, Lovell NH, Dokos S. Simplified 2D bidomain model of whole heart electrical activity and ECG generation. Medical & Biological Engineering & Computing 2013;submitted paper.

[8] Sovilj S, Magjarević R, Lovell NH, Dokos S. Simplified 3D model of whole heart electrical activity and 12-lead ECG generation. Computational and Mathematical Methods in Medicine 2013:Article ID 134208-10.

[9] Sovilj S, Van Oosterom A, Rajsman G, Magjarevic R. ECG based prediction of atrial fibrillation development following coronary artery bypass grafting. Physiological Measurement 2010;31:663-77.

Address for correspondence.

Siniša Sovilj,
University of Zagreb (UNIZG),
Faculty of Electrical Engineering and Computing (FER),
Unska 3, HR-10000 Zagreb, Croatia.
http://hr.linkedin.com/in/ssovilj
sinisa.sovilj@ieee.org